# Facile synthesis of New Polyhedron-like $WO_3$/Butterfly-like $Ag_2MoO_4$ p-n junction photocatalysts with higher photocatalytic activity in UV/Solar region light

Jiabin Liu,[†a] Bowen Yang, [†a] Minghuan Gao, [a] Lisha You,[a] Yuansen Zhang,[a] Zhiying Li,[a] Linna Guo,[a*] Tiesheng Li,[a*], Penglei Chen,[b] and Minghua Liu.[b*]

[a]*College of Chemistry, Zhengzhou University, Zhengzhou, 450001, P. R. China.*

[b]*Beijing National Laboratory for Molecular Science, Institute of Chemistry, Chinese Academy of Sciences, Beijing 100190, P. R China.*

†. These authors contributed equally.

*Corresponding author.
E-mail address: guolinna@zzu.edu.cn; lts34@zzu.edu.cn; liumh@iccas.ac.cn
Tel.: +86-371-67766660 (Office)
Fax.: +86-371-67766667 (Office)

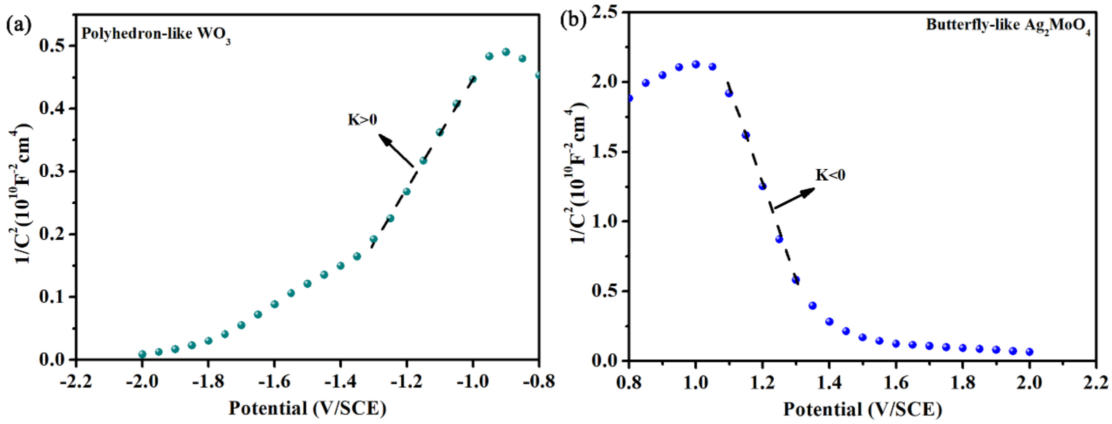


**Fig. S1.** Mott-Schottky cures of (a) Polyhedron-like $WO_3$ and (b) Butterfly-like $Ag_2MoO_4$

In the introduction section, we had mentioned that Polyhedron-like $WO_3$ was most likely an n-type semiconductor [40,41], Butterfly-like $Ag_2MoO_4$ was probably a p-type semiconductor [37,39]. Herein, to further demonstrate the inherent electronic properties of Polyhedron-like $WO_3$, Butterfly-like $Ag_2MoO_4$ and **AWM-20**, Mott-Schottky (M-S) methods were employed to ascertain the semiconductor types of Polyhedron-like $WO_3$ and Butterfly-like $Ag_2MoO_4$ materials. As depicted in Fig. S1, the slope of $1/C^2$ vs potential curves (SCE) over Polyhedron-like $WO_3$ sample was positive, and the slope of $1/C^2$ vs potential cures (SCE) over Butterfly-like $Ag_2MoO_4$ was negative. It was well-known that the positive slope in Mott-Schottky test results was characteristic of n-type semiconductor, while the negative slope represents p-type semiconductor [83,84]. Through to the above experimental results, we could fully prove that Polyhedron-like $WO_3$ material was an n-type semiconductor, $Ag_2MoO_4$ was a p-type semiconductor, when the two semiconductors combined with each other, there would be a p-n junction structure formation.

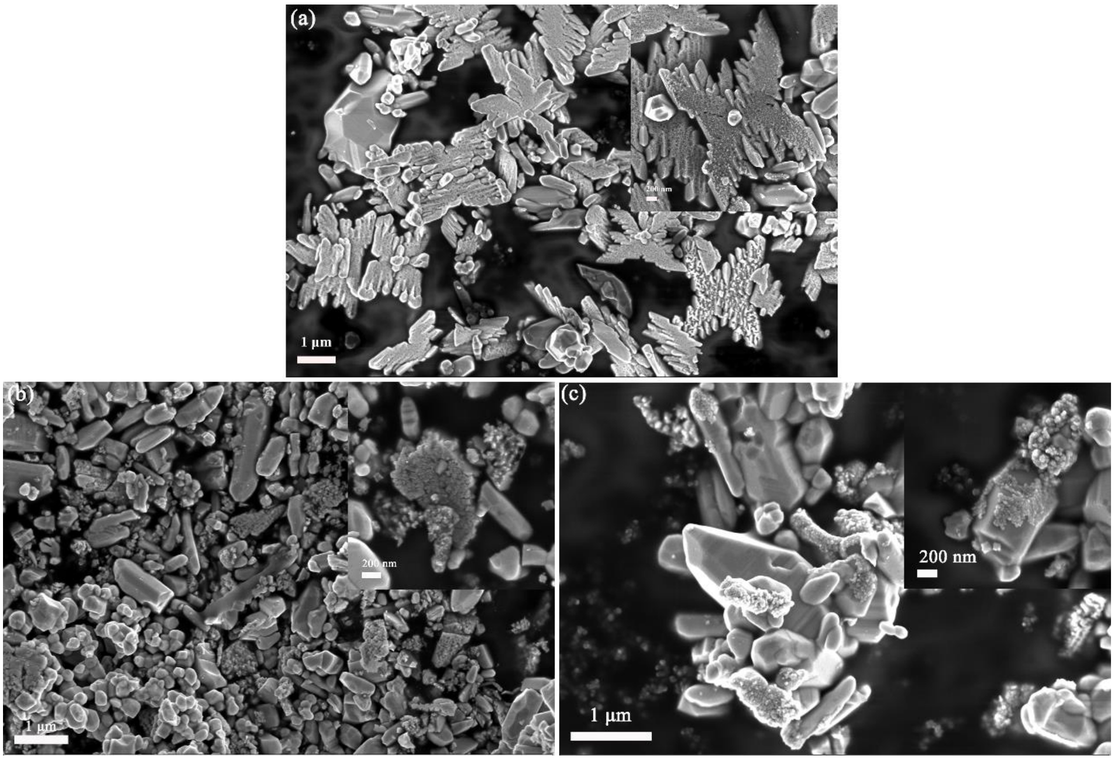


**Fig. S2.** SEM images of (a) fresh AWM-20 sample, (b) used AWM-20 sample after 4 cycling runs under Vis light-driven illumination, (e) used AWM-20 sample after 4 cycling runs under UV light-driven illumination.

**Table. S1.** BET surface areas, pore diameter and pore volumes of the as-prepared samples.

| Photocatalysts | $S_{BET}$ ($m^2g^{-1}$) | Pore diameter (nm) | Pore volume ($cm^3$ $g^{-1}$) |
|---|---|---|---|
| Polyhedron-like $WO_3$ | 2.4734 | 20.8121 | 0.0138 |
| Butterfly-like $Ag_2MoO_4$ | 3.0065 | 8.5451 | 0.0080 |
| AWM-20 | 3.2318 | 16.1415 | 0.0153 |

**Table. S2.** Comparison of Polyhedron-like $WO_3$/Butterfly-like $Ag_2MoO_4$ p-n junction photocatalyst degradation towards organic pollutants (RhB) under visible light. $C_{catalyst}$ is the concentration of photocatalyst in solution, while $C_{pollutants}$ is the concentration of photocatalyst in solution.

| Photocatalysts | $C_{catalyst}$ (mg/mL) | $C_{pollutants}$ (ppm) | Reaction Time (mins) | $K_{app}$ | Refer |
|---|---|---|---|---|---|
| Polyhedron-like $WO_3$/Butterfly-like $Ag_2MoO_4$ p-n junction strcture | 1 | 30 | 18 | 0.2484 | This work |
| Ag@$Ag_2MoO_4$-AgBr composite Plasmonic | 1 | 9.58 | 6 | Not given | 19 |
| cube-like Ag-$Ag_2MoO_4$ | 1 | 9.58 | 80 | Not given | 68 |
| β-$Ag_2MoO_4$/g-$C_3N_4$ heterojunctions catalysts | 0.6 | 5 | 60 | 0.111 | 59 |
| $Ag_2MoO_4$/$Ag_3PO_4$ (AgMoP) composites | 0.5 | 15 | 18 (only 60%) | 0.2401 | 85 |
| Flower-like $Ag_2MoO_4$ /$Bi_2MoO_6$ heterojunctions | 0.6 | 10 | 60 | 0.0435 | 58 |
| Heterostructured $Ag_2MoO_4$/Ag/AgBr cubes | 1 | 15 | 20 | 0.0661 | 67 |

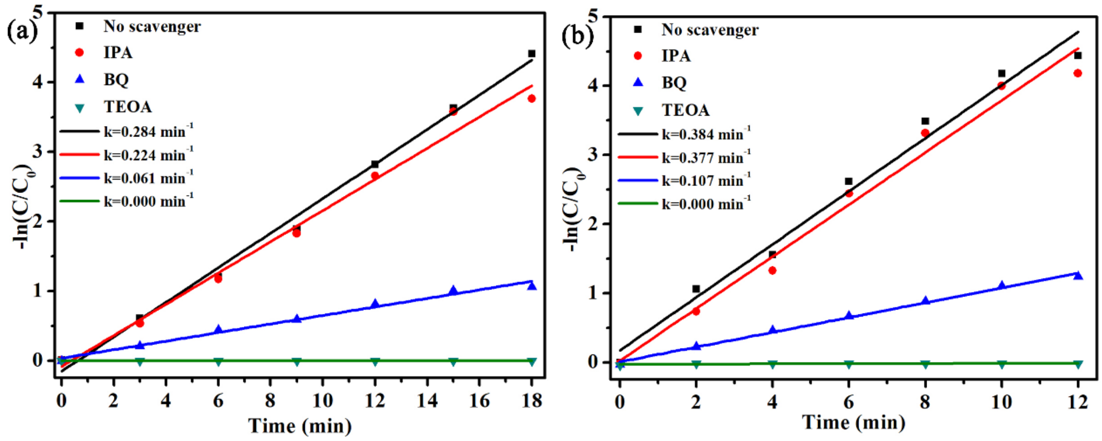


**Fig. S3.** (a) First-order kinetic plots in Fig. 12a for the photodegradation of RhB; (b) First-order kinetic plots in Fig. 12b for the photodegradation of RhB.

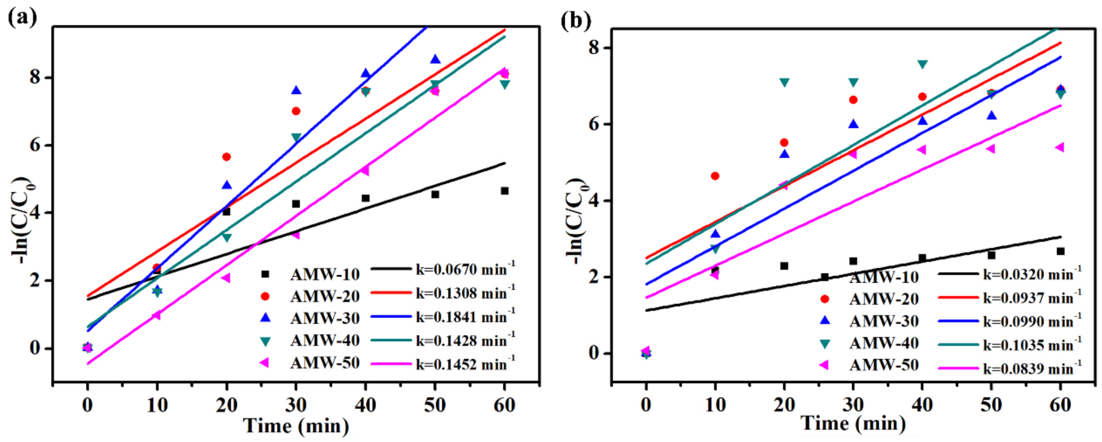


**Fig. S4.** (a) First-order kinetic plots in Fig. 9a for the photodegradation of RhB; (b) First-order kinetic plots in Fig. 9c for the photodegradation of RhB.

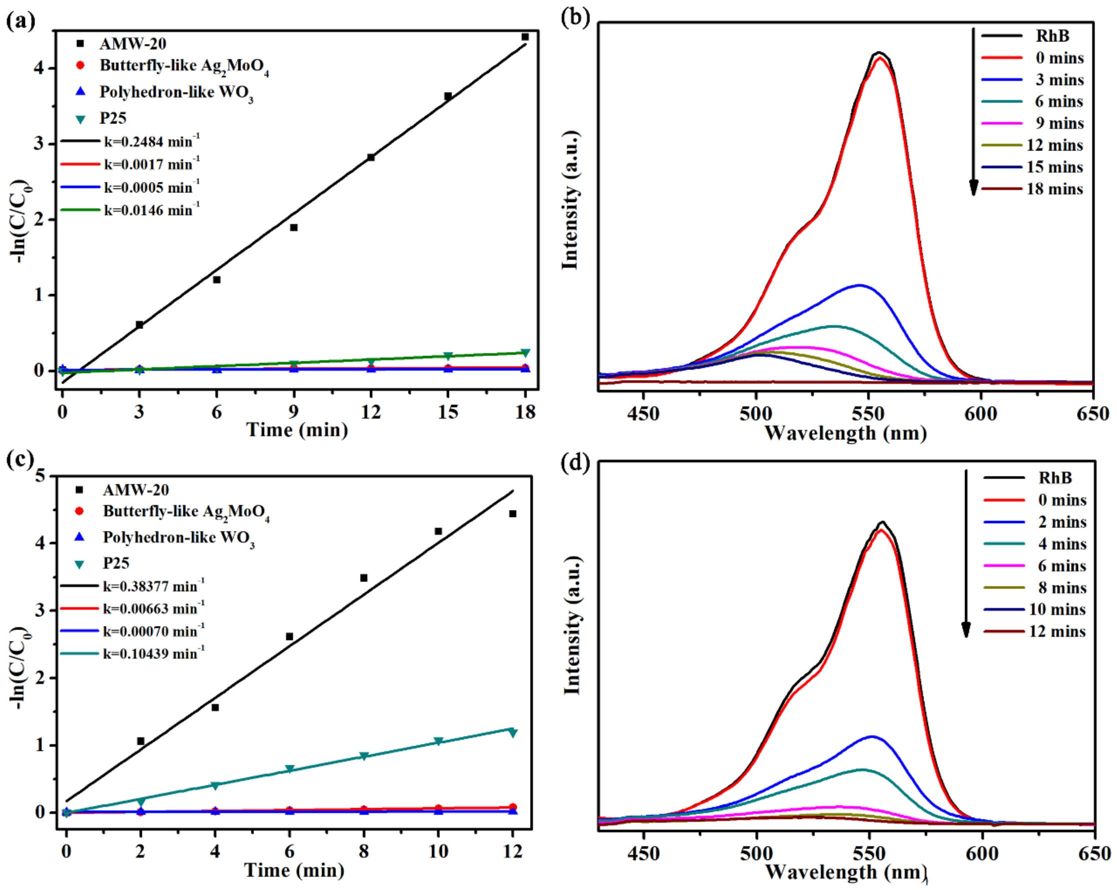


**Fig. S5.** (a) First-order kinetic plots in Fig. 9b for the photodegradation of RhB; (b) The full spectrum of the AWM-20 for RhB degradation under Xe lamp irradiation (Solar); (c) First-order kinetic plots in Fig. 9d for the photodegradation of RhB; (d) The full spectrum of the AWM-20 for RhB degradation under Mercury lamp irradiation (UV).

**Table. S3.** The TON/TOF value of each photocatalyst according to the Fig. 9b.

| Photocatalysts | TON($Ag_2MoO_4$) | TON($WO_3$) | TOF($Ag_2MoO_4$)/min | TOF($WO_3$) | TON(Total) | TOF(Total)/min |
|---|---|---|---|---|---|---|
| Polyhedron-like $WO_3$ | 0.00 | $3.33*10^{-4}$ | 0.00 | $1.85*10^{-5}$ | $3.33*10^{-4}$ | $1.85*10^{-5}$ |
| Butterfly-like $Ag_2MoO_4$ | $8.33*10^{-4}$ | 0.00 | $4.63*10^{-5}$ | 0.00 | $8.33*10^{-4}$ | $4.63*10^{-5}$ |
| AWM-20 | $1.16*10^{-1}$ | $1.79*10^{-2}$ | $6.44*10^{-3}$ | $9.94*10^{-4}$ | $1.34*10^{-1}$ | $7.44*10^{-2}$ |
| P25 | 0.00 | 0.00 | 0.00 | 0.00 | $1.10*10^{-3}$ | $6.11*10^{-5}$ |

**Table. S4.** The TON/TOF value of each photocatalyst according to the Fig. 9d.

| Photocatalysts | TON($Ag_2MoO_4$) | TON($WO_3$) | TOF($Ag_2MoO_4$)/min | TOF($WO_3$) | TON(Total) | TOF(Total)/min |
|---|---|---|---|---|---|---|
| Polyhedron-like $WO_3$ | 0.00 | $2.69*10^{-4}$ | 0.00 | $2.24*10^{-5}$ | $2.69*10^{-4}$ | $2.24*10^{-5}$ |
| Butterfly-like $Ag_2MoO_4$ | $1.81*10^{-3}$ | 0.00 | $1.51*10^{-4}$ | 0.00 | $1.81*10^{-3}$ | $1.51*10^{-4}$ |
| AWM-20 | $1.16*10^{-1}$ | $1.79*10^{-2}$ | $9.67*10^{-3}$ | $1.49*10^{-3}$ | $1.34*10^{-2}$ | $1.12*10^{-3}$ |
| P25 | 0.00 | 0.00 | 0.00 | 0.00 | $3.49*10^{-3}$ | $2.91*10^{-4}$ |

**Table. S5.** The Band energy of $Ag_2MoO_4$ and $WO_3$ calculated by DRS, and UPS.

| Sample | $E_F$(eV) | $E_{VB}$(eV) | $E_{CB}$(eV) |
|---|---|---|---|
| $WO_3$ | -0.76 | 3.72 | 1.00 |
| $Ag_2MoO_4$ | -1.26 | 4.64 | 0.0038 |

**Synthesis of Polyhedron-like $WO_3$ nanoparticles**

Polyhedron-like $WO_3$ nanoparticles were obtained via a hydrothermal process according to our former work [45]. Firstly, concentrated sulfuric acid (98%) was deliquated into aqueous sulfuric acid (3mol/L). Secondly, 3.1870 g of $(NH_4)_6H_2W_{12}O_{40}$ •$xH_2O$ was dissolved in 20 mL deionized water and sonicated for about 10 mins. Subsequently, 6.8 mmol of aqueous sulfuric acid (3 mol/L) was added to the ammonium metatungstate reaction solution. After strongly magnetic stirring for about 30 mins, the above precursor solution was transferred into a 50 mL Teflon-lined stainless-steel autoclave. Next, the reaction autoclave was put in an oven and keep at 180 ℃ for 14 h. Then, the precursor was collected, washed, and dried at 60 ℃ for 12 h. Finally, the prepared precursor was calcined at 700 ℃ for 1 h.

**Synthesis of Butterfly-like $Ag_2MoO_4$ nanoparticles**

Butterfly-like $Ag_2MoO_4$ nanoparticles were synthesized via a facile deposition process according to the previous report [16]. Firstly, 1mmol $CH_3COOAg$ and 0.8325 g

PVP were dissolved it in 50 mL deionized water. Secondly, 2.5 mL $(NH_4)_6Mo_7O_{24}$• $4H_2O$ (0.0285 M) solution was added to the above solution drop by drop, forming a white suspension. Lastly, the Butterfly-like $Ag_2MoO_4$ nanoparticles were synthesized. After centrifugation, the as-obtained samples were washed, dried at 60 ℃ for 12 h.

**Oxidizing organic pollutant progress in direct or indirect way**

The primary process of RhB photodegradation could be inferred as follows:

$$(WO_3/Ag_2MoO_4) + hv \rightarrow e^- + h^+ \quad (1)$$

$$Ag^+ + e^- \rightarrow Ag \quad (2)$$

$$O_2 + e^- \rightarrow \cdot O_2^- \quad (3)$$

$$H_2O + h^+ \rightarrow HO\cdot \quad (4)$$

$$HO\cdot + organic\ pollutant \rightarrow Degraded\ pollutant \quad (5)$$

$$\cdot O_2^- + organic\ pollutant \rightarrow Degraded\ pollutant \quad (6)$$

$$h^+ + organic\ pollutant \rightarrow Degraded\ pollutant \quad (7)$$